Crystal growth and structure analysis of twin-free monoclinic hydroxyapatite

YASUSHI SUETSUGU, JUNZO TANAKA
Advanced Materials Laboratory, National Institute for Materials Science, 1-1 Namiki, Tsukuba, Ibaraki 305-0044, Japan

Single crystals of hydroxyapatite were grown by a flux method using $Ca_3(PO_4)_2$ and $Ca(OH)_2$ under 100 MPa of Ar gas. The crystals obtained had stoichiometric composition of $Ca_{10}(PO_4)_6(OH)_2$ and some of them were twin-free single crystals. From X-ray diffraction analyses, the space group was confirmed to be monoclinic $P2_1/b$ with cell parameters $a = 0.9419(3)$ nm, $b = 1.8848(6)$ nm, $c = 0.6884(2)$ nm, and $\gamma = 119.98(2)^\circ$. The detailed crystal structure was determined with a reliability factor $R_w = 0.033$; the O atoms of OH were located just on the 2_1 axis while the H atoms of OH occupied the positions a little deviated from the 2_1 axis. The origin of this structure was ascribed to the formation of hydrogen bonds between the H atoms of the OH ions and the specific O atoms of the PO_4 ions.

1. Introduction

The crystal structure of hydroxyapatite (HAp) has been studied by many researchers, and the positions of Ca and PO_4 ions were elucidated in detail [1–4]. However, the occupation site and configuration of OH ions are still unsettled though they are of importance for the comprehension of crystal growth and bone regeneration mechanisms, further especially for the development of novel biocompatible implants. This is just due to difficulty in procuring large single crystals sufficient for X-ray diffraction analysis.

Small single crystals of HAp have been synthesized under hydrothermal conditions [5–12]. For example, rod-shaped crystals of 8 mm in length and 0.5 mm across were obtained by a hydrothermal flux method [10, 11], and large crystals of $7 \times 3 \times 3\,mm^3$ in size with a stoichiometric composition were grown using retrograde solubility of HAp [12]. Single crystals of HAp have been prepared also by heating flux-grown chlorapatite (ClAp) crystals in steam at 1300 °C for two weeks; then, Cl ions were substituted with OH ions [13].

The structure analyses of HAp have been carried out on the basis of the space group $P6_3/m$ of fluorapatite (FAp) [1–3]. However, as regards stoichiometric HAp, its space group was ascribed to monoclinic $P2_1/b$ as well as ClAp [14]. The fundamental structure of $P2_1/b$ is as follows: OH ions are located a little off the *b*-glide planes, and the directions of O–H axes are parallel to the *c*-axis. As there are two positions for the OH ions that are alternately occupied, the periodicity along the *b*-direction is double the *a*-axis.

Up to the present, the structural analyses of stoichiometric HAp were performed to understand the role of the OH ions in the HAp structure; nevertheless there has been no report except for that by Elliott *et al*. [4] using monoclinic but twinned crystals [13]. In this paper, therefore, the details of the monoclinic HAp structure are described using stoichiometric twin-free HAp crystals grown by a flux method.

2. Experimental procedure

2.1. Crystal growth of HAp

Starting materials, tricalcium phosphate ($Ca_3(PO_4)_2$, TCP) and $Ca(OH)_2$, were prepared as follows: First, brushite ($CaHPO_4 \cdot 2H_2O$) powder was synthesized by reacting $CaCO_3$ (Ube Materials, $> 99.99\%$) with phosphoric acid (Wako, 85%) diluted with water, and was heated at 800 °C in the air for 2 h to make β-$Ca_2P_2O_7$. Then, α-TCP powder was obtained by heating the mixture of β-$Ca_2P_2O_7$ and the equal mole of $CaCO_3$ at 1300 °C for 1 h. As for $Ca(OH)_2$, $CaCO_3$ powder was heated in the air at 1050 °C for 3 h, and the CaO obtained was hydrated with pure water during the cooling process; the reaction temperature was about 200 °C.

A mixture of 25 mol % of TCP and 75 mol % of $Ca(OH)_2$ powders was packed in a Pt tube of 10 mm in diameter and 50 mm in length. A metal piston was used in packing to avoid leak due to the excessive deformation of the tube during a high-pressure process, and the tube was sealed by carbon arc welding.

HAp crystals were grown under an Ar gas pressure of about 100 MPa using a high-pressure vessel equipped with Pt–Rh heater (Mitsubishi Heavy Industries, Ltd.). The sample was heated up to 1450 °C, and after 2 h the temperature was lowered to 1100 °C by 5 °C/h. The pressure deviation was suppressed at about $\pm 5\%$ around the pressure set. After the growth, the sample was rapidly cooled by about 30 °C/min until 800 °C. The residual flux was removed by immersing in 10 wt % of EDTA-Na_2 aqueous solution for five days.

The crystals obtained were analyzed by an electron probe microanalyzer (EPMA: JEOL JXA-8600MX) using oxide ZAF compensation: the accelerating voltage and beam current were 15 kV and 10 nA, respectively. A wollastnite ($CaSiO_3$) crystal and a sintered stoichiometric HAp were used as standard samples.

2.2. X-ray diffraction analysis

A specimen with hexagonal prismatic morphology of $140 \times 140 \times 160\,\mu m^3$ in size was selected from the twin-free crystals obtained to measure the X-ray diffraction. The diffraction measurement was achieved at room temperature with a four-circle diffractometer (Rigaku Co. Ltd., AFC-5R) using AgKα radiation of 40 kV and 180 mA (a rotating anode tube, monochrometer: pyrolitic graphite, detector slit width: 1/2°). The AgKα X-ray was used to detect H because its absorption effect is small, though the short wavelength is unfavorable against measuring diffractions from a large cell parameter, *b*. The space group, in addition the existence of twinning, was elucidated from the X-ray reflections along *h*01, 0*k*1 and $-hh1$ on the first layer in a reciprocal space.

X-ray diffraction data were collected in the range of $4° \leq 2\theta \leq 70°$ corresponding to $0 \leq h \leq 19$, $-30 \leq k \leq 30$ and $-14 \leq l \leq 14$ using a ω-2θ scan technique: a scan rate in 2θ was $8° \,min^{-1}$. A total of 8892 independent reflections were measured, and 7401 reflections with intensities larger than σ were used for the structural analysis. Lattice parameters were refined by a least-square method using 25 2θ-values measured.

The refinement of the crystal structure was undertaken using a program of Xtal 3.4 [15]; equivalent reflection data were averaged using Fisher test, and a weighing factor for the data observed was $1/\sigma^2(F)$. Atomic scattering factors for neutral atoms and anomalous dispersion factors were cited from Ibers and Hamilton [16]. In the calculations, initial positions for Ca, and P and O of PO_4 were taken from the previous results [4]. After refining the positional parameters of Ca, and P and O of PO_4 tetrahedra, the positions of OH ions were determined by means of difference Fourier (D-Fourier) electron density maps. Finally, the positions of all the constituents were simultaneously refined by a full-matrix least-square method.

3. Results and discussion

3.1. HAp crystals grown by a flux method

A phase diagram utilizable for the TCP–$Ca(OH)_2$ system was investigated by Biggar [8] in a temperature range 700–950 °C at 100 MPa, and the crystal growth of HAp using a reaction $3Ca_3(PO_4)_2 + Ca(OH)_2 \rightarrow Ca_{10}(PO_4)_6(OH)_2$ was carried out on the basis of the equilibrium phase relation [10, 11]. However, the phase diagram was inapplicable to the present crystal growth because its liquidus line was quite steep and the existence of the monoclinic phase was vague. The crystal growth conditions were therefore surveyed by trial and error in a high content region of TCP and in a high temperature region. The optimal condition was given at 25 mol % TCP and at a temperature from 1100 to 1450 °C.

Fig. 1 shows the monoclinic HAp single crystal obtained. The morphology is of hexagonal prism with caps of hexagonal pyramid, elongated in the *c*-axis direction; the largest crystals reached the size of 7 mm in length and 1 mm in diameter. As a Ca/P ratio was determined to be 1.67(1) from EPMA analyses, the chemical formula of the crystals was $Ca_{10}(PO_4)_6(OH)_2$ without defects.

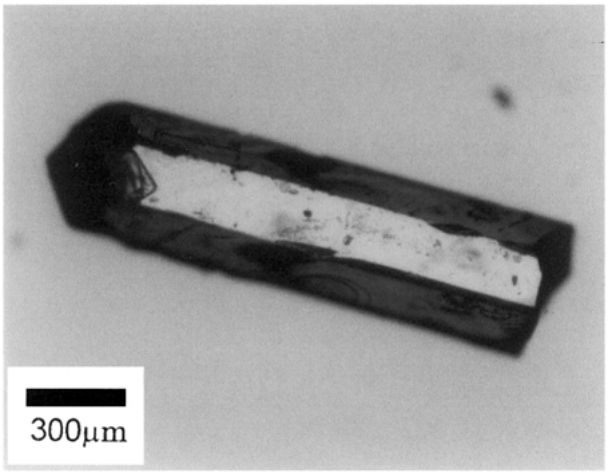

Figure 1 Stoichiometric HAp crystal synthesized in the TCP–$Ca(OH)_2$ system.

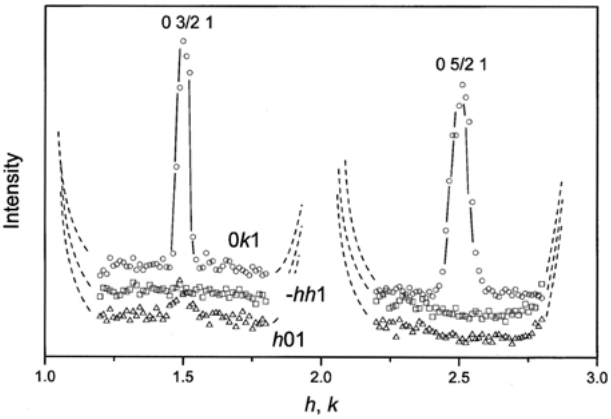

Figure 2 X-ray diffraction intensity scanned along *h*01, 0*k*1 and $-hh1$ on the first layer of HAp crystal. The indices are given for the hexagonal system. Extremely strong peaks are removed from the data, leaving gaps.

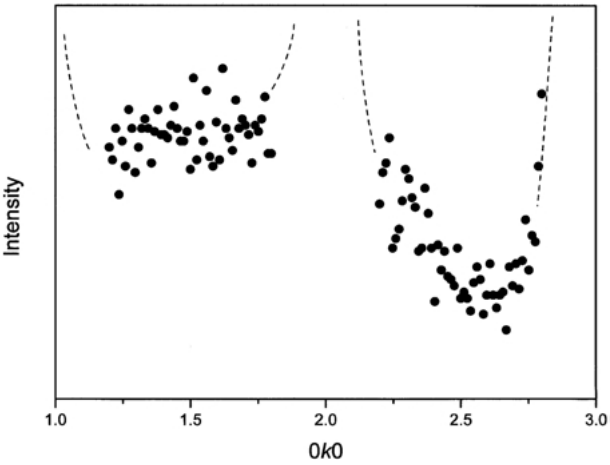

Figure 3 X-ray diffraction intensity scanned along 0*k*0 of HAp crystal. The indices are given for the hexagonal system. Extremely strong peaks are removed from the data, leaving gaps.

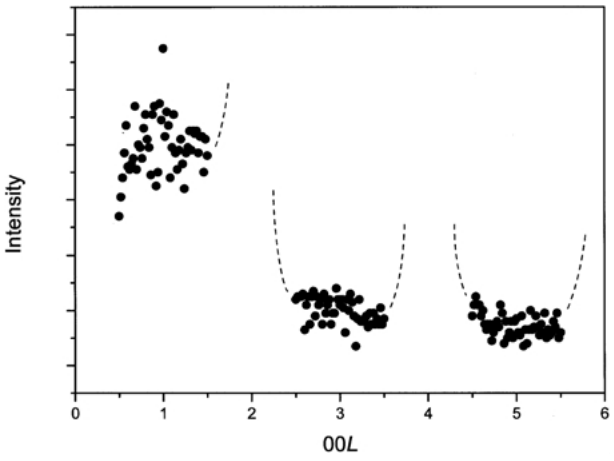

Figure 4 X-ray diffraction intensity scanned along the *c**-axis of HAp crystal. Extremely strong peaks are removed from the data, leaving gaps.

3.2. Determination of space group

In order to select twin-free crystals, the intensity distribution of X-ray diffraction was measured with a four-circle diffractometer. Fig. 2 indicates the intensity distributions along $h01$, $0k1$ and $-hh1$ on the first layer of $hk1$ in a reciprocal space. Here, the diffraction indices are, for simplicity, given on the basis of the hexagonal system. The peaks at $(0, 3/2, 1)$ and $(0, 5/2, 1)$ (open circles) are very intense, while no peak is found at $(-3/2, 3/2, 1)$ and $(-5/2, 5/2, 1)$ (squares) nor at $(3/2, 0, 1)$ and $(5/2, 0, 1)$ (triangles). This result indicates that the *b*-axis should be twice as long as that of the hexagonal cell. Therefore, this single crystal is monoclinic without twinning. As regards $0k0$ on the zeroth layer in the reciprocal space (Fig. 3), there is no peak at $(0, 3/2, 0)$ nor at $(0, 5/2, 0)$, indicating the existence of a *b*-glide plane. Further, since an extinction rule of $00l$ $(l = 2n + 1)$ is valid from an intensity distribution along the *c**-axis as shown in Fig. 4, there exists a screw axis 2_1 in this space group. Consequently, the space group of the crystal is $P2_1/b$. Cell parameters were $a = 0.9419(3)$ nm, $b = 1.8848(6)$ nm, $c = 0.6884(2)$ nm, and $\gamma = 119.98(2)^\circ$.

TABLE I Positional parameters of HAp

	x	*y*	*z*	B_{eq}
Ca(1)	0.32641(6)	0.58033(3)	0.00081(7)	0.97(1)
Ca(1′)	0.34044(6)	0.58694(3)	0.49779 (7)	0.91(1)
Ca(2a)	0.24599(6)	0.24649(3)	0.25293(7)	0.86(1)
Ca(2b)	−0.00670(6)	0.62305(3)	0.74424(7)	0.85(1)
Ca(2c)	0.25397(6)	0.37346(3)	0.75590(7)	0.85(1)
P(a)	0.63125(7)	0.26521(4)	0.25469(9)	0.65(2)
P(b)	0.02971(7)	0.44896(4)	0.75148(9)	0.66(2)
P(c)	0.39787(7)	0.43419(4)	0.25468(9)	0.66(2)
O(1a)	0.4842(2)	0.32788(11)	0.7583(3)	1.06(5)
O(1b)	0.1567(2)	0.58605(12)	0.2465(3)	1.04(5)
O(1c)	0.3278(2)	0.49213(12)	0.2592(3)	1.06(5)
O(2a)	0.5345(2)	0.31112(11)	0.2437(3)	1.22(6)
O(2b)	0.1220(2)	0.54334(11)	0.7334(3)	1.13(6)
O(2c)	0.5863(2)	0.48253(12)	0.2377(3)	1.14(6)
O(3a)	0.7465(2)	0.29076(12)	0.0785(3)	1.41(6)
O(3b)	0.0792(3)	0.41302(14)	0.5820(3)	1.40(6)
O(3c)	0.3278(3)	0.37519(12)	0.0820(3)	1.33(6)
O(3′a)	0.7376(2)	0.29506(12)	0.4376(3)	1.18(6)
O(3′b)	0.0893(2)	0.42890(12)	0.9401(3)	1.18(6)
O(3′c)	0.3565(3)	0.38223(12)	0.4399(3)	1.16(6)
O(4)	−0.0003(2)	0.25007(13)	0.3034(4)	1.19(6)
H	−0.005(4)	0.253(2)	0.437(6)	2.37(158)

3.3. Structure analysis using four-circle X-ray diffraction data

Fig. 5 shows the D-Fourier contour map of the $x = 0$ section calculated for a structure model consisted of only Ca and PO_4 ions. The electron density takes maximal values at $(0, 0.25, 0.2)$, $(0, 0.25, 0.3)$, and their equivalent positions. The largest peak at $(0, 0.25, 0.3)$ corresponds to the OH ion while the weak peak at $(0, 0.25, 0.2)$ is ascribed to the small amount of OH ions due to a partially formed domain structure. The site occupancy of the latter

TABLE II Anisotropic thermal parameters of HAp

	U_{11}	U_{22}	U_{33}	U_{12}	U_{13}	U_{23}
Ca(1)	0.0138(2)	0.0147(2)	0.00830(18)	0.00718(17)	0.00022(15)	−0.00041(15)
Ca(1′)	0.0128(2)	0.0157(2)	0.00810(17)	0.00856(17)	0.00006(15)	−0.00045(15)
Ca(2a)	0.01187(17)	0.01270(19)	0.00975(16)	0.00734(14)	−0.00021(16)	0.00011(16)
Ca(2b)	0.01130(17)	0.0125(2)	0.00964(16)	0.00681(14)	−0.00024(15)	0.00036(15)
Ca(2c)	0.01113(17)	0.0131(2)	0.00943(16)	0.00706(14)	−0.00017(15)	0.00028(15)
P(a)	0.0096(2)	0.0098(2)	0.0073(2)	0.00637(19)	−0.0002(2)	0.0002(2)
P(b)	0.0090(2)	0.0094(2)	0.0075(2)	0.00516(18)	−0.0003(2)	−0.0003(2)
P(c)	0.0084(2)	0.0109(2)	0.0075(2)	0.00602(19)	−0.0006(2)	−0.0002(2)
O(1a)	0.0186(8)	0.0153(8)	0.0122(7)	0.0130(7)	−0.0001(6)	0.0003(6)
O(1b)	0.0151(7)	0.0105(7)	0.0126(7)	0.0054(6)	0.0009(6)	−0.0003(6)
O(1c)	0.0090(6)	0.0192(8)	0.0129(7)	0.0077(6)	0.0005(6)	−0.0004(7)
O(2a)	0.0124(7)	0.0148(8)	0.0204(9)	0.0077(6)	0.0030(7)	0.0007(7)
O(2b)	0.0125(7)	0.0131(8)	0.0213(9)	0.0094(6)	−0.0012(7)	0.0002(7)
O(2c)	0.0133(7)	0.0094(7)	0.0210(9)	0.0057(6)	0.0012(6)	0.0017(6)
O(3a)	0.0316(12)	0.0162(9)	0.0107(7)	0.0158(9)	−0.0073(7)	−0.0033(6)
O(3b)	0.0144(9)	0.0192(10)	0.0127(8)	0.0033(7)	0.0055(6)	−0.0016(6)
O(3c)	0.0181(9)	0.0281(11)	0.0125(8)	0.0176(9)	−0.0028(6)	−0.0067(7)
O(3′a)	0.0199(9)	0.0175(9)	0.0111(7)	0.0122(7)	0.0033(6)	0.0048(6)
O(3′b)	0.0151(8)	0.0158(9)	0.0106(7)	0.0054(7)	−0.0033(6)	0.0016(6)
O(3′c)	0.0147(8)	0.0204(10)	0.0109(7)	0.0102(7)	0.0001(6)	0.0029(6)
O(4)	0.0103(8)	0.0128(9)	0.0222(11)	0.0058(7)	−0.0010(6)	−0.0025(7)

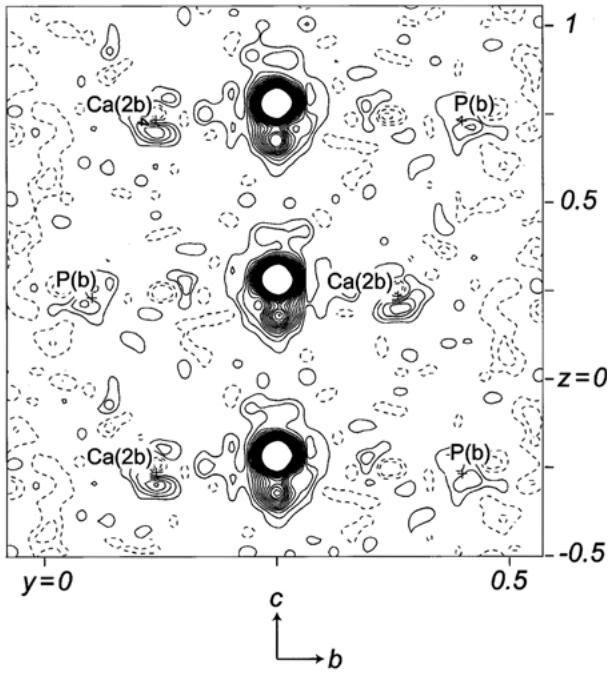

Figure 5 D-Fourier map of the (1 0 0) plane for the present HAp crystal after the refinement for Ca and PO_4 group without OH. The contour is at an interval of $5 \times 10^2\,nm^{-3}$. Solid and broken lines correspond to positive and negative contours, respectively. Atom positions within 0.03 nm from this plane are given.

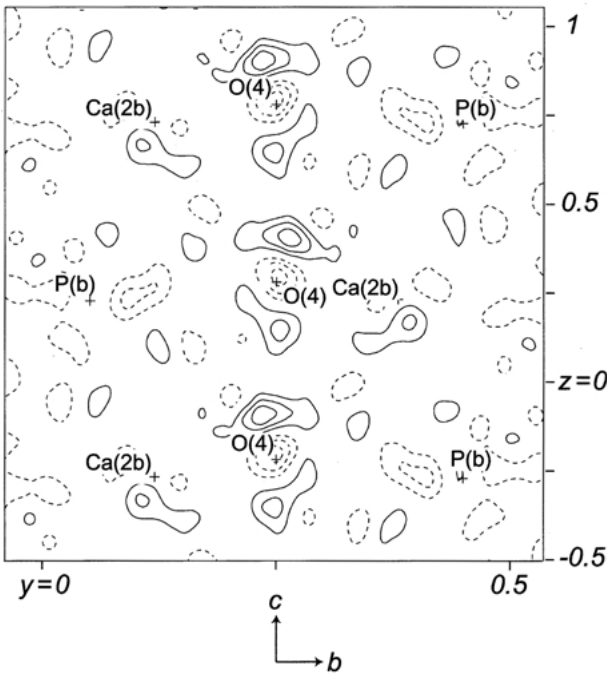

Figure 6 D-Fourier map of the (1 0 0) plane for the present HAp crystal after the refinement for Ca, PO_4 group and hydroxy O without H. The contour is at an interval of $2 \times 10^2\,nm^{-3}$. Solid and broken lines correspond to positive and negative contours, respectively. Atom positions within 0.03 nm from this plane are given.

OH ions is so small that the symmetry is not practically influenced. In this figure, the H atom cannot be found.

Fig. 6 shows the D-Fourier map obtained for the structure model in which the O atoms of OH ions were added but without H atom. This D-Fourier map was synthesized using the reflections having $\sin\theta/\lambda$ values less than 0.6 to enhance the contribution of H atom,

TABLE III Bond lengths and angles in the HAp structure (The parameters calculated on the basis of hexagonal symmetry are cited from Hughes *el al*. [3].)

	HAp	HAp (hexagonal)
P(a)–O(1a)	0.1535(2)	0.1534
P(a)–O(2a)	0.1541(3)	0.1537
P(a)–O(3a)	0.1536(2)	0.1529
P(a)–O(3′a)	0.1531(2)	
P(b)–O(1b)	0.1536(2)	
P(b)–O(2b)	0.1546(2)	
P(b)–O(3b)	0.1534(3)	
P(b)–O(3′b)	0.1535(2)	
P(c)–O(1c)	0.1533(3)	
P(c)–O(2c)	0.1542(2)	
P(c)–O(3c)	0.1533(2)	
P(c)–O(3′c)	0.1535(2)	
O(1a)–P(a)–O(2a)	111.27(12)	111.04
O(1a)–P(a)–O(3a)	110.94(12)	111.43
O(1a)–P(a)–O(3′a)	111.51(11)	
O(2a)–P(a)–O(3a)	108.00(13)	107.51
O(2a)–P(a)–O(3′a)	107.23(13)	
O(3a)–P(a)–O(3′a)	107.71(11)	107.73
O(1b)–P(b)–O(2b)	111.08(14)	
O(1b)–P(b)–O(3b)	110.57(11)	
O(1b)–P(b)–O(3′b)	111.51(11)	
O(2b)–P(b)–O(3b)	109.07(12)	
O(2b)–P(b)–O(3′b)	106.68(11)	
O(3b)–P(b)–O(3′b)	107.78(15)	
O(1c)–P(c)–O(2c)	111.05(12)	
O(1c)–P(c)–O(3c)	110.48(14)	
O(1c)–P(c)–O(3′c)	112.05(13)	
O(2c)–P(c)–O(3c)	108.71(13)	
O(2c)–P(c)–O(3′c)	106.87(12)	
O(3c)–P(c)–O(3′c)	107.52(11)	
O(1a)–O(2a)	0.2539(3)	0.2531
O(1a)–O(3a)	0.2530(2)	0.2531
O(1a)–O(3′a)	0.2534(2)	
O(2a)–O(3a)	0.2489(4)	0.2473
O(2a)–O(3′a)	0.2473(3)	
O(3a)–O(3′a)	0.2477(3)	0.2471
O(1b)–O(2b)	0.2542(2)	
O(1b)–O(3b)	0.2523(3)	
O(1b)–O(3′b)	0.2539(3)	
O(2b)–O(3b)	0.2508(3)	
O(2b)–O(3′b)	0.2472(3)	
O(3b)–O(3′b)	0.2479(3)	
O(1c)–O(2c)	0.2535(4)	
O(1c)–O(3c)	0.2519(3)	
O(1c)-O(3′c)	0.2544(4)	
O(2c)–O(3c)	0.2500(3)	
O(2c)–O(3′c)	0.2471(3)	
O(3c)–O(3′c)	0.2474(3)	
Ca(2c)–Ca(2a)	0.4082(1)	0.4085
Ca(2a)–Ca(2a)	0.4089(1)	
Ca(2b)–Ca(2c)	0.4080(2)	

because the scattering factor of H atom is valid only for such small $\sin\theta/\lambda$. In Fig. 6, a small but apparent peak is observed at $(0, 0.27, 0.4)$: its electron density is $8 \times 10^2\,nm^{-3}$. A distance between the O atom of OH ion and the small peak is about 0.09 nm. As this value is quite equal to the ordinary O–H distance, it is considered that the peak $(0, 0.27, 0.4)$ corresponds to the H atom of the OH ion.

Fig. 7 shows the D-Fourier contour map at $x = 0$ calculated for the overall model including the H atoms of OH ions by a full-matrix least-square method. The resultant weighed *R*-factor was 0.033, and only small residue remains less than $6 \times 10^2\,nm^{-3}$. This result

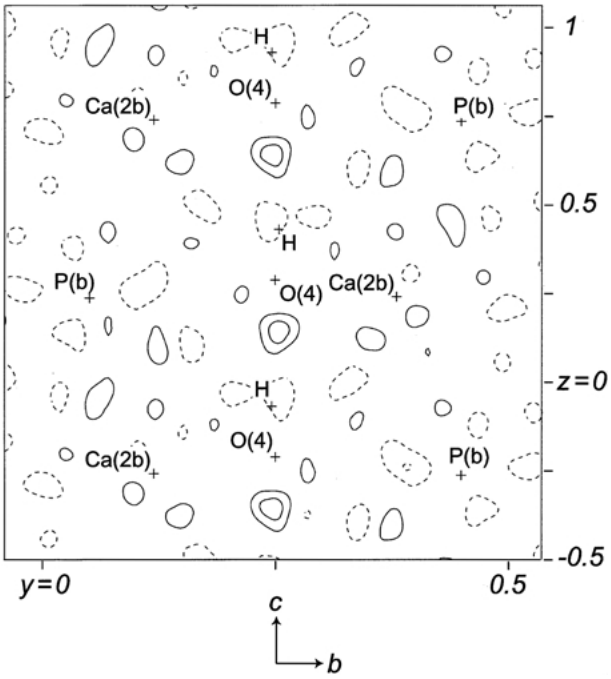

Figure 7 D-Fourier map of the (1 0 0) plane for the present HAp crystal after the refinement for Ca, PO_4 group and OH. The contour is at an interval of 2×10^2 nm^{-3}. Solid and broken lines correspond to positive and negative contours, respectively. Atom positions within 0.03 nm from this plane are given.

indicates that the structural model is appropriate for the present HAp crystal. Table I gives the final positional parameters obtained, and anisotropic thermal parameters are listed in Table II. Table III gives bond lengths and angles calculated. Figs 8 and 9 show the atomic configuration projected on (1 0 0) and (0 0 1) planes, respectively.

The most remarkable changes of the monoclinic HAp from the hexagonal HAp are the deviation of the H atom of the OH ion from the 2_1 axis, and the corresponding shift of O(3) and O(3′) of PO_4 ion. The origin of these behaviors is plausibly due to the formation of hydrogen bonds between the H atoms of the OH ions and the O(3) and O(3′) atoms of the PO_4 ions. As shown in Fig. 10, the distances of H–O(3a), H–O(3b) and H–O(3c) are 0.3075, 0.2903 and 0.2958 nm, and the corresponding distances of H–O(3′a), H–O(3′b) and H–O(3′c) are 0.2923, 0.3091 and 0.3036 nm, respectively. The distances of H–O(3b) and H–O(3′a) are significantly shorter in comparison with the others, indicating that the chemical bond formed between the H–O pairs.

4. Conclusions

Single crystals of HAp were successfully grown by a flux method using the mixture of TCP and $Ca(OH)_2$. The

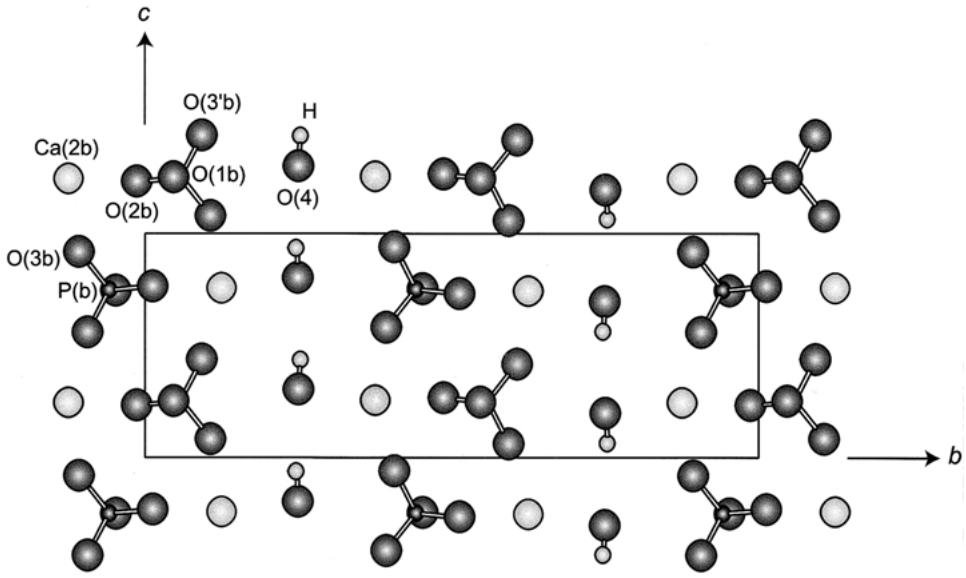

Figure 8 The atomic configuration in HAp projected on the (1 0 0) plane.

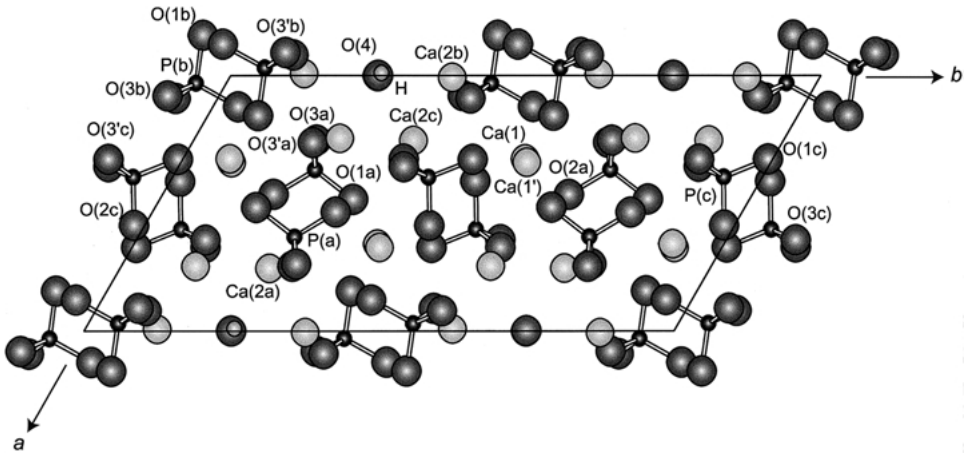

Figure 9 The atomic configuration in HAp projected on the (0 0 1) plane.

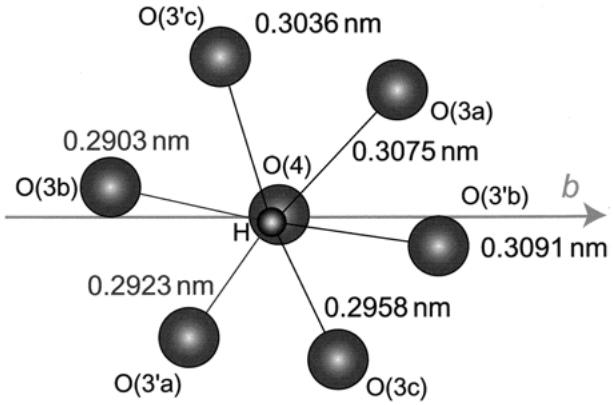

Figure 10 Distances between hydroxy H and O(3)s of PO_4 in HAp.

crystals obtained were hexagonal prismatic and the size of the largest crystal was about 7 mm in length and 1 mm in diameter. The composition was stoichiometric $Ca_{10}(PO_4)_6(OH)_2$.

X-ray structure analysis of HAp using a twin-free monoclinic single crystal was performed and precise location of the H atom of the OH ion was determined. The location of the H atom was slightly deviated from 2_1 axis, indicating relatively intense bonds between the H atoms and the O(3b) and O(3′a) atoms of the PO_4 ions.

References

1. A. F. POSNER, A. PERLOFF and A. F. DIORIO, *Acta Cryst.* **11** (1958) 308.
2. M. I. KAY, R. A. YOUNG and A. S. POSNER, *Nature* **204** (1964) 1050.
3. J. M. HUGHES, M. CAMERON and K. D. CROWLEY, *Amer. Mineralogist* **74** (1989) 870.
4. J. C. ELLIOTT, P. E. MACKIE and R. A. YOUNG, *Science* **180** (1973) 1055.
5. A. PERLOFF and A. S. POSNER, *ibid.* **124** (1956) 583.
6. W. HAYEK, W. BOHLER, J. LECHLUTNER and H. Z. PETTER, *Z. Anorg. Alig. Chem.* **295** (1958) 241.
7. H. JULLMANN and R. MOSEBACH, *Z. Naturforsch.* **21b** (1966) 493.
8. G. M. BIGGAR, *Mineral. Mag.* **35** (1966) 1110.
9. J. F. KIRN and H. LEIDHEISER, *J. Cryst. Growth* **2** (1968) 111.
10. D. M. ROY, *Mat. Res. Bull.* **6** (1971) 1337.
11. W. EYSEL and D. M. ROY, *J. Cryst. Growth* **20** (1973) 245.
12. M. MENGEOT, M. L. HARVILL, O. R. GILLIAM and E. KOSTINER, *ibid.* **19** (1973) 199.
13. J. C. ELLIOTT and R. A. YOUNG, *Nature* **214** (1967) 904.
14. J. C. ELLIOTT, *Nat. Phys. Sci.* **230** (1971) 72.
15. S. R. HALL, G. S. D. KING and J. M. STEWART, ''Xtal 3.4 User's Manual'' (University of Western Australia, 1995).
16. J. A. IBERS and W. C. HAMILTON, in ''International Tables for X-ray Crystallography'', vol. IV (Kynoch Press, Birmingham, 1974).

Received 14 July
and accepted 22 October 2001